

# Investigation of the Synthesis, Characterization and Properties of Nano $\text{Cu}_2\text{Zr}_3\text{O}_7$ – HDPE Composite Sheets

Jammula Koteswara Rao<sup>1\*</sup>, J.S. Sagar<sup>1</sup>, G.M. Madhu<sup>1</sup> and Dixit Pradipkumar<sup>2</sup>

1. Department of Chemical Engineering, MS Ramaiah Institute of Technology, Bangalore -560 054, Karnataka, INDIA

2. Department of Electrical and Electronics Engineering, M. S. Ramaiah Institute of Technology, Bangalore 560054, INDIA

\*koteswararao@msrit.edu

## Abstract

*This study reports on the synthesis of  $\text{Cu}_2\text{Zr}_3\text{O}_7$  nanoparticles using the solution combustion method followed by the fabrication and characterization of micro-composite sheets of  $\text{Cu}_2\text{Zr}_3\text{O}_7$  - HDPE. The characterization was performed using SEM, XRD and EDX analysis which demonstrated the effects of nano-sized  $\text{Cu}_2\text{Zr}_3\text{O}_7$  particles on the crystallinity and surface morphology of the fillers and elemental analysis using the EDX method. The dielectric behavior of the composite was investigated using an Impedance Analyzer. The composite's tensile strength was increased as evidenced by 34% increase in Young's modulus compared to blank HDPE for the sample with 1.5 wt% nanofiller loading.*

*The results indicated that the dielectric constant increased as the frequency decreased, with higher values observed at 10 MHz. However, this trend was less pronounced at reduced filler loadings. The loss tangent initially dropped abruptly and then gradually as the frequency increased between 4 Hz and 1 MHz. The addition of  $\text{Cu}_2\text{Zr}_3\text{O}_7$  nanoparticles resulted in increased conductivity at higher frequencies compared to pure HDPE, with no significant frequency dependency observed at lower frequencies.*

**Keywords:** HDPE, Copper Zirconium oxide, Electrical properties, Mechanical Properties.

## Introduction

The concept of "nano sandwiches" was first published in an article in Chemistry. Nature has been utilizing the mixing of nanoparticles and polymers such as fats, proteins, simple and complex carbohydrates to create solid composites such as shells, wood and bones. These nanocomposites are prepared by incorporating more than one phase such as layers or fibres and particles where at least one of the phases is in the nanometre range. The properties of these materials are influenced not only by the properties of the nanofillers, but also by their interfacial and morphology characteristics.<sup>2</sup>

Nanofillers such as carbon nanotubes, copper, titania, zinc, silica and layered silicates are being studied for their ability to significantly alter the mechanical and electrical properties of polymeric matrices. Polymer composites are currently manufactured commercially for a wide range of applications, including sporting goods, aerospace components,

automobiles and more. The final product does not have to be in the nanoscale, but can be in the micro or macroscopic size range.<sup>17</sup>

Novel materials are being developed in the field of polymers, despite the fact that polymeric materials have excellent resistance to chemicals, are inexpensive, are quickly synthesized, have fouling qualities, electrical features and mechanical attributes. The high-density polyethylene is one of the oldest and most widely used thermoplastic material. (HDPE). One of the most significant mechanical attributes to consider is the electromechanical reaction. There may be some disadvantages to polyethylene such as creep resistance and weak stiffness as well as inadequate temperature stability. The use of modest amounts of nanofillers (usually less than 10% by weight) into polyethylene has been shown to successfully boost creep strength.<sup>1,8</sup>

The addition of smoked silica particles with uniform scattering at low nanofiller content into a high-density polyethylene (HDPE) matrix was achieved through melt compounding process. The nanofillers used had various surface properties and sizes. The nanofillers' surface area and HDPE matrix dispersion were improved according to analysis applying field emission scanning electron microscopy. The thermo-mechanical properties of the nanocomposites were found to be improved compared to pure HDPE. Both dimensional stability and thermal degradation resistance were increased. The mechanical properties, such as stress-strain break, were also enhanced with the addition of 2 vol% of nano-particles into the HDPE matrix. The tensile stress and elastic modulus at yield were improved, indicating enhanced polymer-filler interfacial interaction.<sup>24</sup>

CuO nanoparticles (CuNPs) are synthesized through an electrodeposition process. These nanoparticles are known for their anti-corrosive properties as well as their thermal conductivity and lightweight characteristics. These nanoparticles are then integrated into HDPE matrix after they have been developed. As a result of properties like as chemical inertness, minimal permeability to moisture, high processability and superior rigidity, HDPE has received a lot of attention. The melt mixing process was used to manufacture varied concentrations of Cu-HDPE nanocomposites using a twin-screw extruder.

Surface morphological characteristics of these nanocomposite films were analyzed using SEM and observations revealed that there were no defects discovered on the film' surfaces and CuNPs were spread evenly.<sup>21</sup> The modulus of

traditional polymer compositions loaded with bigger fillers typically increases linearly with the filler weight fraction.

However, in the case of nanomaterials, even modest filler concentrations can result in a large and quick rise in modulus, outperforming conventional fillers.<sup>5</sup> This behavior can be explained by the presence of an impacted polymer layer on the filler surface, which has a significantly greater Young's modulus than the bulk equivalent polymer. This polymer is the portion of the polymer matrix that is physisorption on the nanofiller surfaces, resulting in reinforcement and enhanced affinity for adherence to the filler surfaces.<sup>22</sup>

Zirconia oxide (ZrO<sub>2</sub>) NPs were synthesized using the thermal pressing technique. Nanocomposites were made by combining ZrO<sub>2</sub> NPs with HDPE and changing the NP concentration. Later, the effects of nanocomposites were studied employing characterization techniques as XRD, DSC, TGA etc. The results of XRD illustrate that the ZrO<sub>2</sub> nanoparticles and HDPE have not changed their crystalline structure after being added to the polymer. SANS investigation shows that they are evenly dispersed in an HDPE matrix. DSC testing revealed that melting point dropped and crystallinity amount increased. The effect of gamma radiation was examined by TGA and DTG analysis. The addition of nanofiller into HDPE composite lowered the decomposition temperature. When related to the ZrO<sub>2</sub>-water system as well, the effect may be explained by moving the radiation energy received by the NPs and then continuing resonant inductive interaction to neighbouring polymer molecules.<sup>3,5</sup>

Zirconia oxide and hydroxyapatite, two nanofillers with the varying concentrations, were added to the polymer blending by 5:95 (HDPE:PMMA) during melt process (single screw extruder). SEM technology was used to study the surface morphology of the synthesized polymer mix nanocomposite, which reveals the diverse morphologies at varying concentrations. Two different types of mix composites were made in order to examine the impact of mechanical properties.

When compared to hydroxyapatite blend composites, zirconia blend composites had most favourable outcomes. When compared to zirconia blend composites, hydroxyapatite blend composites containing nano-fillers showed an increase in resistance to wear.<sup>19,22</sup>

The intended effect of the present investigation is to synthesize copper zirconium oxide nanoparticles employing a solution burning technique using urea, sugar and glycine as suitable sources of energy. The SEM, XRD and EDX methods were used for studying these nanomaterials.

Subsequently, nano copper zirconium oxide-HDPE composite films with various loadings of nanofillers were developed. From that, we evaluated the mechanical and electrical properties of fabricated nano copper - zirconium oxide and HDPE composite films.

## Material and Methods

**Materials:** The zirconyl nitrate (AR grade) used in the experiments was supplied by Loba Chemie, Mumbai, India and had a purity of >45%. Cupric nitrate trihydrate, glycine and urea were purchased from Merck India and SD Fine-Chem Limited (SDFCL) with a purity of 95-103% and >99% respectively. Commercially available sugar (C<sub>12</sub>H<sub>22</sub>O<sub>11</sub>) and high-density polyethylene (HDPE) with a melt flow index of 4 g/10 min were procured from Saraswathi Plastics, Bangalore, India. Double distilled water (DDW) was used throughout the procedure.

## Synthesis of Cu<sub>2</sub>Zr<sub>3</sub>O<sub>7</sub> Nanoparticles

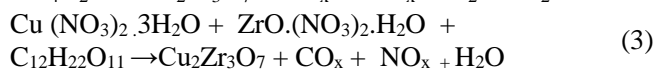
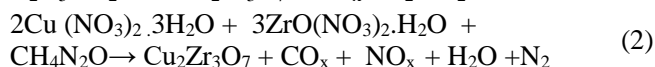
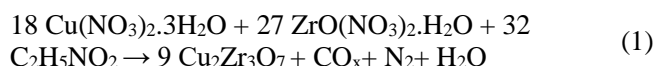
**Solution Combustion Method:** The materials used in the synthesis, including cupric nitrate, zirconyl nitrate and fuel (glycine, urea, or sugar), were measured and transferred into a beaker in the quantities shown in table 1 for a yield of 5 g of product. The mixture was homogenized by adding 100 mL of deionized water and stirring until a uniform solution was obtained. The reaction mixture was then transferred to a Muffle furnace and heated to 400°C for 2 hours. After cooling for a few minutes, the resulting combustible product was ground and placed back into the Muffle furnace for calcination at 600°C for 30 minutes. The final product obtained was a black powdery material consisting of copper zirconium oxide nanoparticles.

The oxidizer-to-fuel (O/F) ratio and the fuel type are important variables that affect a combustion synthesis reaction. In order to calculate the O/F ratio, equation 1 can be used to express the oxidizing valency of any metal nitrate. The fuel to oxidant ratio of 0.3 had been chosen in order to ensure optimum fuel combustion whereas the oxidizer was present. Equation 2.2 displays the reaction stoichiometry according to this ratio.

**Table 1**  
Reagents quantity required for the synthesis of Cu<sub>2</sub>Zr<sub>3</sub>O<sub>7</sub>

Fuel Source	Fuel Required (gm)	Cupric Nitrate Required (gm)	Zirconyl Nitrate Required (gm)
Glycine	1.099	4.71	6.76
Urea	0.88	4.71	6.76
Sugar	4.98	4.71	6.76

For continuing the chemical reaction at a mole ratio of 0.3 of copper oxide to fuel, the nitrate is completely burnt, leaving no carbon residue behind. In addition, the reaction releases its maximum quantity of energy.



### Fabrication of nanoCu<sub>2</sub>Zr<sub>3</sub>O<sub>7</sub> - HDPE polymer composites:

To synthesize the polymer nanocomposite specimens, the weight % of nano Cu<sub>2</sub>Zr<sub>3</sub>O<sub>7</sub> added to the HDPE matrix was varied from 0.5 to 2.5. The blend preparation and compression molding steps were carried out to make the nano Cu<sub>2</sub>Zr<sub>3</sub>O<sub>7</sub>-HDPE composites. For blend preparation, HDPE granules and nano Cu<sub>2</sub>Zr<sub>3</sub>O<sub>7</sub> particles were weighed and mixed in a 100 mL beaker. Aminosilane was added slowly while continuously stirring to complete 4 mL of the binding substance. The mixture was blended in a Brabender melt mixer for five minutes at a constant plate temperature of 130°C and a rotating speed of 10 rpm. The resulting mixture was then compressed into sheets of 15 cm x 15 cm using a hot press at 130°C and 80 bar pressure for 10 and 20 minutes of heating and curing time respectively. The compatible substance concentration was held constant at 4 mL for all polymer composites.

**Characterization Techniques:** Characterization tools in comprehending the physical and chemical properties of polymer nanocomposites (PNCs) are essential for researching new materials and providing information on intrinsic properties. Commonly used analysis methods are wide-angle X-ray diffraction (XRD), Scanning electron microscopy (SEM) and Transmission electron microscopy (TEM).<sup>11, 23</sup> The mechanical and electrical properties of the nanocomposite films were evaluated and compared to those of pure HDPE. The study was carried out using an ASTM-compliant Universal Testing Machine (UTM model: KIPLPC 2000; error range: 0.2 MPa; test speed for holding surface: 10 mm/min; load cell: 0.2 kN) as per ASTM standards. A high frequency LCR meter (Agilent 4294 A) with an intensity between 40 Hz to 110 MHz was used to evaluate the electrical properties of the nanocomposite sheets. These techniques enable researchers to collect data on the physical and chemical properties of polymer nanocomposites, which are critical for understanding their performance and potential applications.

### Results and Discussion

Cu<sub>2</sub>Zr<sub>3</sub>O<sub>7</sub> nanoparticles were synthesized using three different fuel sources: glycine, urea and sugar. These nanoparticles will be characterized using SEM, XRD and EDX techniques to learn more about their structural, morphological and elemental properties. HDPE will be blended with Cu<sub>2</sub>Zr<sub>3</sub>O<sub>7</sub> nanoparticles and the resulting

polymer nanocomposite sheets will be surface modified with aminosilane.<sup>7</sup> Aminosilane is a common coupling agent that improves the interfacial interaction between nanoparticles. The finding will provide important insights into the potential of Cu<sub>2</sub>Zr<sub>3</sub>O<sub>7</sub> nanoparticles as a reinforcement material for HDPE, as well as impact on the mechanical and dielectric properties of polymer nanocomposites.

### Characterization Techniques

**SEM Analysis:** The Cu<sub>2</sub>Zr<sub>3</sub>O<sub>7</sub> nanoparticles were SEM analysed (TESCAN VEGA 3 LMU Scanning electron microscope) with magnifications ranging from 10,000X to 68,800X and a working distance of approximately 5 mm. The secondary electron detector was used for analysis and because the samples were inherently non-conductive, they were coated with gold for 60 seconds before SEM analysis using a Quorum sputtering unit.

The particle distribution and surface morphology of the synthesised Cu<sub>2</sub>Zr<sub>3</sub>O<sub>7</sub> nanoparticles were revealed by SEM images. The particle surface morphology was clearly visible in fig. 1a, fig. 2a and fig. 3a. As shown in fig. 1b, the smallest particle size measured was 30.56 nanometres. As shown in fig. 1b, fig. 2b and fig. 3b, the average particle size for the synthesised nanoparticles was 80 nm for the glycine sample, 120 nm for the urea sample and 130 nm for the sugar sample. The urea-fueled synthesis of Cu<sub>2</sub>Zr<sub>3</sub>O<sub>7</sub> nanoparticles demonstrated the most uniform particle distribution with particles of similar size among the three samples. The morphology and particle size of all three samples appeared to be mostly uniform. It is also noticeable that the particles tend to fragment, straightening out the oxide film from bulk particles.

**XRD Analysis:** The Cu<sub>2</sub>Zr<sub>3</sub>O<sub>7</sub> nanoparticles were analyzed using X-ray diffraction (XRD) with glycine, urea and sugar as fuel samples. The objective of the study was to identify the zirconium oxide (ZrO<sub>2</sub>) and copper oxide (CuO) in the samples. The XRD patterns obtained from the three samples (glycine, urea and sugar) clearly showed the presence of ZrO<sub>2</sub> and CuO characteristic peaks. Five major individual diffraction peaks were observed at 2θ values around 31, 35.5, 38.8, 52 and 61.5° in fig. 4a, fig. 4b and fig. 4c, which were also compared with the standard file (JCPDS file no. 48-1548).<sup>15</sup> The crystalline nature of pure CuO nanoparticles was identified by these patterns.<sup>9</sup>

Furthermore, a series of XRD peaks were observed at two values near 30, 35, 38, 50 and 60° which were identified as diffractions of cubic phase ZrO<sub>2</sub> (JCPDS card no. 49-1642).<sup>13</sup> The zirconium oxide peak was observed at 2θ = 29° in all three samples, with the glycine and sugar samples having the highest peak. As shown in fig. 4b and fig. 4c, the highest copper oxide peak was observed in the urea sample at 2θ = 30°, while it was the second highest peak in the glycine and sugar samples. These study results confirmed the presence of CuO in the ZrO structure, resulting in the formation of Cu<sub>2</sub>Zr<sub>3</sub>O<sub>7</sub> nanoparticles.

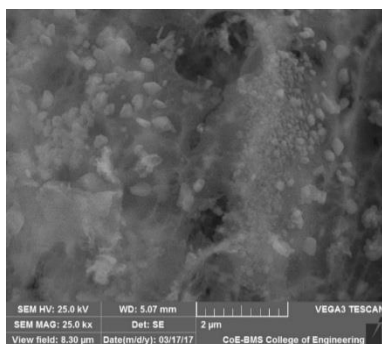


**Fig. 1a:** SEM image of nano  $\text{Cu}_2\text{Zr}_3\text{O}_7$  particles using glycine (25000X)

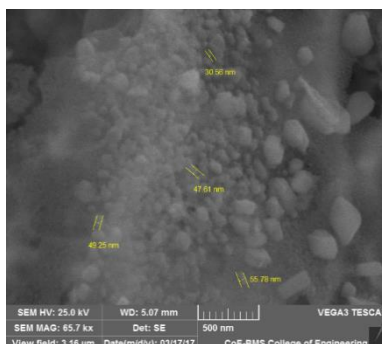


**Fig. 1b:** SEM image of nano  $\text{Cu}_2\text{Zr}_3\text{O}_7$  particles using glycine (65700X)

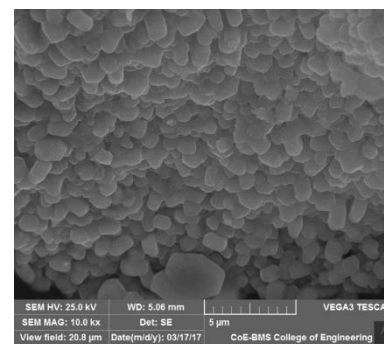


**Fig. 2a:** SEM image of nano  $\text{Cu}_2\text{Zr}_3\text{O}_7$  particles using urea (10000X)

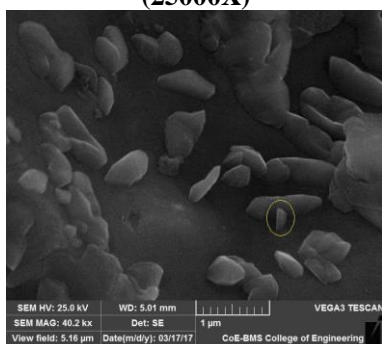


**Fig. 2b:** SEM image of nano  $\text{Cu}_2\text{Zr}_3\text{O}_7$  particles using urea (45200X)

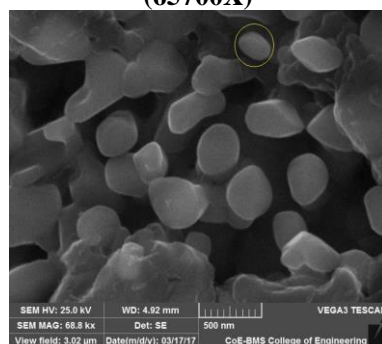


**Fig. 3a:** SEM image of nano  $\text{Cu}_2\text{Zr}_3\text{O}_7$  particles using sugar (15000X)

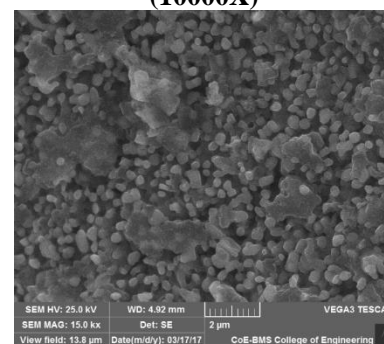


**Fig. 3b:** SEM image of nano  $\text{Cu}_2\text{Zr}_3\text{O}_7$  particles using sugar (68800X)

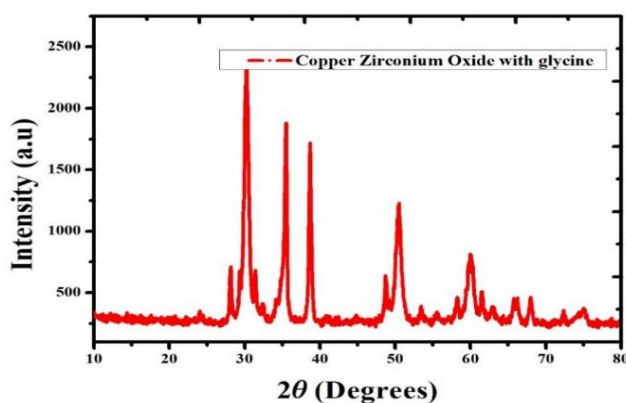


**Fig. 4a:** XRD profile of nano  $\text{Cu}_2\text{Zr}_3\text{O}_7$  particles using glycine

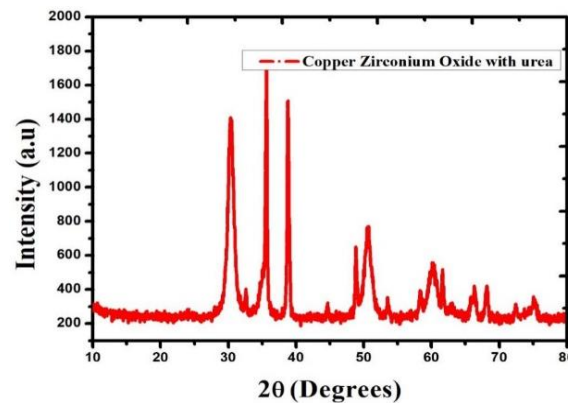


**Fig. 4b:** XRD profile of nano  $\text{Cu}_2\text{Zr}_3\text{O}_7$  particles using urea

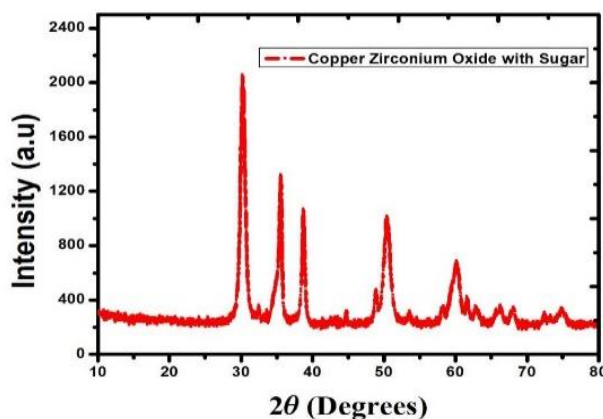


**Fig. 4c:** XRD profile of nano  $\text{Cu}_2\text{Zr}_3\text{O}_7$  particles using sugar

**Energy Dispersive X-Ray Spectroscopy (EDX) Analysis:**

EDAX AMETEK was used to analyse the EDX spectra of synthesised nano  $\text{Cu}_2\text{Zr}_3\text{O}_7$  particles are shown in fig. 5a, fig. 5b and fig. 5c. The prerequisites for analysis were the same as for SEM. The objective of the energy dispersive X-ray spectroscopy (EDX) profiles was to perform elemental analysis or chemical characterization on a sample. The elemental analysis of the samples showed the inclusions of copper, zirconium and oxygen in the nanoparticles as shown in fig. 5a, fig. 5b and fig. 5c. EDX spectra show that the percentage of composition in  $\text{Cu}_2\text{Zr}_3\text{O}_7$  NPs is unreliable. It varies from point to point, indicating that the composition of the synthesised NPs is not identical and it reinforces the SEM analysis.

SEM and EDX scanning were used to perform structural analysis to better understand the elemental distribution on the surface of the nano  $\text{Cu}_2\text{Zr}_3\text{O}_7$  particles (EDX analysis). The SEM images showed that the particles were sintered and had a higher density. The EDX analysis revealed the composition of  $\text{ZrO}_2$  particles and a  $\text{CuO}$  matrix, which were linked to elemental O, Zr and Cu peaks respectively. The nano  $\text{ZrO}_2$  particles were discovered to have a higher melting point, greater hardness and excellent thermal stability. At high temperatures, the nanoparticles were observed to harden and increase the composite strength at the melting point of copper.<sup>12</sup>

**Mechanical Properties:** Tensile properties of nano  $\text{Cu}_2\text{Zr}_3\text{O}_7$  - HDPE composite sheets were investigated with

a Tensometer (Zwick Roell, ZHU 2.5) equipped with Instron tensile flat surface grips. For testing purposes, the composite sheets were sliced into 1 cm wide strips of the same length using a bandsaw cutter. For each variation in the blend's composition, a minimum of three specimens were tested and the results were averaged for analysis.

Tensile testing was performed at a crosshead speed of 2 mm/min, which refers to the rate at which the Tensometer's crosshead moves during the test. This speed determines the strain rate that the material experiences during the tensile test and it can have an effect on the mechanical properties of the material. Tensile properties that were typically measured include tensile strength, yield strength, elongation at break and modulus of elasticity. These properties describe material's ability to withstand tensile forces, deform under stress and return to its original shape after the load is removed. Tensile testing results can be used to assess the mechanical performance of nano  $\text{Cu}_2\text{Zr}_3\text{O}_7$  - HDPE composite sheets and their suitability for specific applications.

**Stress strain curves analysis:** Fig. 6 illustrates the stress-strain curves of nano  $\text{Cu}_2\text{Zr}_3\text{O}_7$  - HDPE composites. All samples went through an elastic deformation phase followed by a nearly monotonically increasing stress during plastic deformation until failure. However, as shown in table 2, different mechanical properties serve as a function of varying  $\text{Cu}_2\text{Zr}_3\text{O}_7$  concentration.

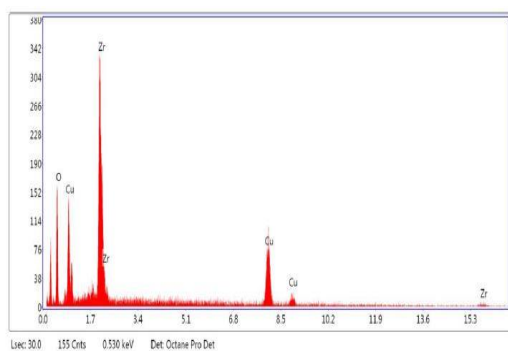


Fig. 5a: EDX profile of nano  $\text{Cu}_2\text{Zr}_3\text{O}_7$  particles using glycine

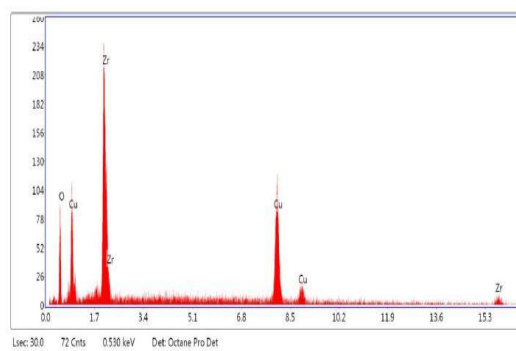


Fig. 5b: EDX profile of nano  $\text{Cu}_2\text{Zr}_3\text{O}_7$  particles using urea

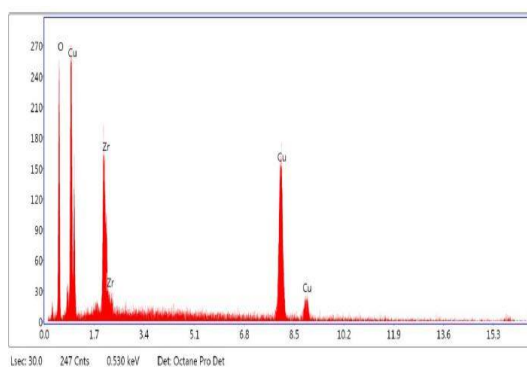


Fig. 5c: EDX profile of nano  $\text{Cu}_2\text{Zr}_3\text{O}_7$  particles using sugar

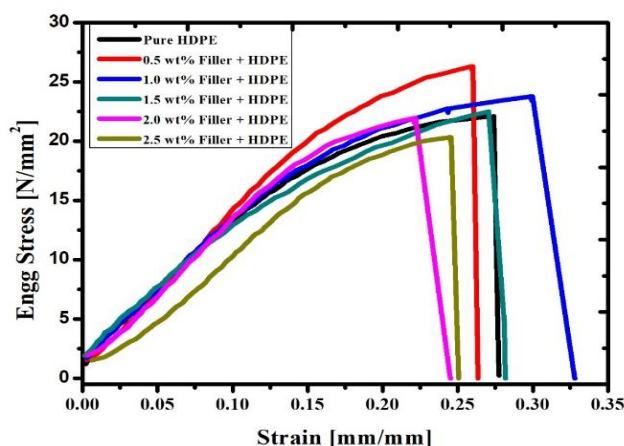


Fig. 6: Stress vs strain curves as a function of nano  $\text{Cu}_2\text{Zr}_3\text{O}_7$  loaded HDPE sheets concentration of  $\text{Cu}_2\text{Zr}_3\text{O}_7$  in weight%: (a) 0.0 (b) 0.5 (c) 1.0 (d) 1.5 (e) 2 (f) 2.5 for different filler content.

Table 2

Various mechanical properties as a function of varying  $\text{Cu}_2\text{Zr}_3\text{O}_7$  Loading (by wt%)

Filler Loading (wt %)	Young's Modulus (MPa)	% Young's Modulus	Ultimate Tensile Strength (MPa)	% Ultimate Tensile Strength	Toughness ( $\text{J}/\text{mm}^2$ )
0	103.94	-	21.86	-	4.11
0.5	134.95	29.83	26.30	20.31	4.26
1	128.97	24.08	23.78	8.78	4.79
1.5	124.77	20.04	22.51	3.11	4.05
2	123.36	18.68	21.95	0.04	3.25
2.5	116.83	12.40	20.33	-	2.98

**Young's modulus:** Table 2 illustrates the behaviour of Young's modulus, stress-at-break and strain-at-break as a function of filler loading. As revealed in fig. 7, the Young's modulus of HDPE sheets filled with  $\text{Cu}_2\text{Zr}_3\text{O}_7$  nanoparticles improved linearly with increasing filler loading. The inclusion of 0.5 weight percent  $\text{Cu}_2\text{Zr}_3\text{O}_7$  nanoparticles increased the Young's modulus from 103.94 to 134.95 MPa. This implies that the addition of nano  $\text{Cu}_2\text{Zr}_3\text{O}_7$  particles improves Young's modulus, which gradually increases with increasing filler concentration, confirming the stiffening impact of the filler on HDPE due to the high Young's modulus of the filler fraction. However, at low filler concentration, the polymer nanocomposites showed only a small improvement in tensile strength, as indicated by the results. This shows that the mechanical property improvements could be related to strong hydrogen bonding interactions between the nano filler and the HDPE matrix.<sup>18</sup>

**Ultimate Tensile Strength:** The behavior of ultimate tensile strength, which is closely related to Young's modulus, was studied for the nano  $\text{Cu}_2\text{Zr}_3\text{O}_7$ -HDPE composites. Fig. 8 illustrates that the tensile strength improves slightly (about 20%) for filler loading up to 5%. However, the results indicate a substantial decrease in tensile strength after loading more than 5% filler, with the values becoming relatively constant as filler content increases further. This suggests that the addition of 0.5 wt.%  $\text{Cu}_2\text{Zr}_3\text{O}_7$  nanoparticles to the HDPE matrix can strengthen the

molecular interface, resulting in an increase in Young's modulus and a slight improvement in yield strength.

However, excessive nano filler loading may result in a decrease in tensile strength, indicating that there may be an optimal loading level for achieving the desired mechanical properties in nano  $\text{Cu}_2\text{Zr}_3\text{O}_7$ -HDPE composites.

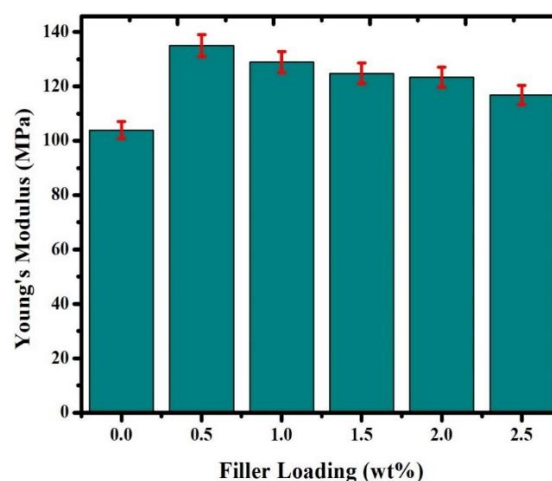
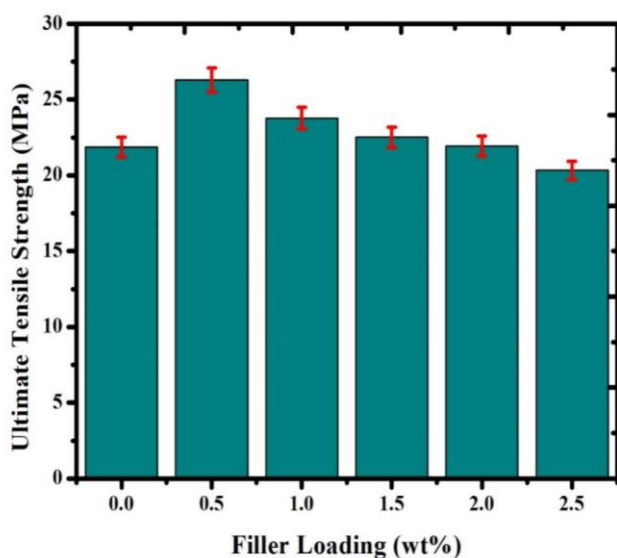


Fig. 7: Variation of Young's modulus with  $\text{Cu}_2\text{Zr}_3\text{O}_7$  filler loading in HDPE

The incorporation of nanofillers and cross-linking was found to be responsible for the improvement in tensile strength.

Cross-linking, which refers to the development of chemical links between polymer chains, results in a stronger and more rigid material. On the other hand, the incorporation of nanofillers can form a relatively weak nanofiller-matrix boundary, which acts as crack-stopping mechanisms during the early stages of fracture propagation, ultimately slowing the formation of the main crack.<sup>16</sup>

According to the findings, the compact strengthening of nanofillers within the HDPE matrix allows load transfer from the fillers to the matrix via the polymer-matrix boundary, resulting in improved mechanical properties and a higher dielectric constant, which can be significant for potential applications. However, some variations in the results may be attributed to factors such as solvent residue holes and nanofiller clustering within the matrix. The tensile strength data shows the interfacial interactions between HDPE and nano  $\text{Cu}_2\text{Zr}_3\text{O}_7$  particles. The ultimate tensile strength increases first at low filler loading and subsequently declines significantly with increasing filler content up to 2.5 wt.%, with the ultimate tensile strength being 26.30 MPa which is 20% of the original strength.



**Fig. 8: Variation of ultimate tensile strength with  $\text{Cu}_2\text{Zr}_3\text{O}_7$  filler loading in HDPE**

**Toughness:** Fig. 9 exhibits the difference in toughness of nano  $\text{Cu}_2\text{Zr}_3\text{O}_7$  - HDPE composites as a function of nano filler content. The use of nanofillers reduces the toughness of the polymer nanocomposites. The results show that toughness drops from 4.11  $\text{J}/\text{mm}^2$  for pristine HDPE to 2.98  $\text{J}/\text{mm}^2$  for the polymer composite with 2.5 wt% filler content. The highest toughness was measured at 1.0 wt% filler content, with a value of 4.79  $\text{J}/\text{mm}^2$  and it lowers further as filler concentration increases.

The decreased toughness is due to an improper interfacial connection between the filler material and the matrix. As the filler content increases, the capacity of the nanoparticles to bend decreases, affecting the stretching behaviour of the composite resulting in a decrease in toughness. This implies

that the mechanical properties of the nanocomposite are influenced by the interfacial interactions between the nanofillers and the matrix and that a higher filler concentration can result in lower toughness.<sup>6</sup>

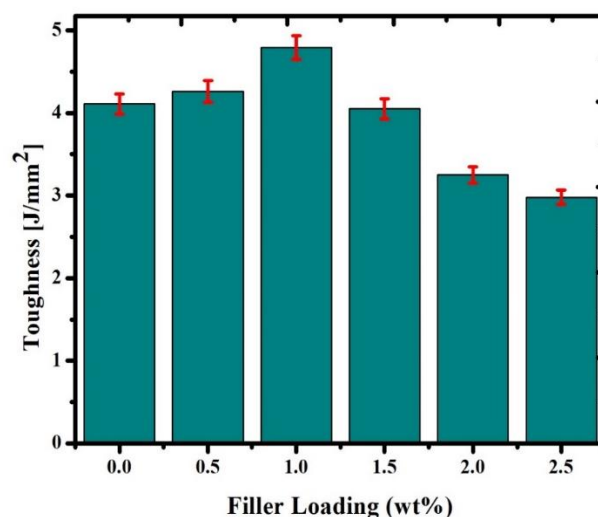


**Fig. 9: Variation of toughness with  $\text{Cu}_2\text{Zr}_3\text{O}_7$  filler loading in HDPE**

**Dielectric Properties Analysis:** The dielectric characteristics of nano  $\text{Cu}_2\text{Zr}_3\text{O}_7$  - HDPE composite sheets were measured using electrical testing. The sheets were cut into  $1\text{cm} \times 1\text{cm}$  squares for study and the dielectric characteristics of the samples were measured using an Impedance Analyzer (Agilent Technologies, Japan).

The effective dielectric permittivity of nanocomposites is determined by the dielectric behaviour of the composite material, which involves polarization from HDPE and  $\text{Cu}_2\text{Zr}_3\text{O}_7$  nanoparticles as well as interfacial polarization at the interfaces between HDPE and nanoparticles. The high-volume fraction of interfaces in the produced nanocomposites is expected to result in interfacial polarizations.<sup>4,10,14,20</sup>

The dielectric characteristics of nano  $\text{Cu}_2\text{Zr}_3\text{O}_7$  - HDPE composite sheets were measured throughout a frequency range of 4 Hz to 1 MHz, as well as the capacitance  $C_p$  (in Farad) and loss tangent. By employing eq. 4 and eq. 5, the dielectric constant ( $\epsilon_r$  or  $\epsilon^*$ ) and dielectric loss ( $\epsilon''$ ) values were computed from the capacitance and loss tangent. Fig. 10 and fig. 11 show the frequency-dependent values of  $\epsilon'$  and  $\tan \delta$  for the composite sheets at various filler concentrations.

The dielectric behaviour of the composite sheets as a function of frequency is described by the complex permittivity which is given by eq. 4

$$\epsilon^* = \epsilon'(\omega) - i\epsilon''(\omega) \quad (4)$$

The real part of the complex permittivity,  $\epsilon'(\omega)$ , represents the energy storage component, while the imaginary part,

$\varepsilon''(\omega)$ , represents the energy loss component in each cycle of the electric field. The measured capacitance ( $C_p$ ) was used to calculate the dielectric constant  $\varepsilon'(\omega)$  using eq. 5:

$$\varepsilon' = \frac{C_p \times t}{A \times \varepsilon_0} \quad (5)$$

where  $\varepsilon_0$  is the permittivity of air ( $8.85 \cdot 10^{-12}$  F/m),  $t$  is the thickness of the film in [m],  $A$  is the sample surface area in [m<sup>2</sup>],  $\omega$  is the angular frequency in [s<sup>-1</sup>] given by  $\omega = 2\pi f$  and  $f$  is frequency in [s<sup>-1</sup>]. In contrast, eq. 6 gives the dielectric loss  $\varepsilon''(\omega)$ .

$$\varepsilon''(\omega) = \varepsilon'(\omega) \times \tan\delta(\omega) \quad (6)$$

where  $\tan\delta(\omega)$  is the loss tangent, the thickness (mean value 2.30 mm) and area (1.9 cm<sup>2</sup>) of the samples evaluated in the impedance analyzer.

**Dielectric constant:** Fig. 10 depicts the dielectric constant ( $\varepsilon'$ ) of nano  $\text{Cu}_2\text{Zr}_3\text{O}_7$  - HDPE composites as a function of log frequency. At lower frequencies, dielectric permittivity tends to be higher, which could be due to sample interfacial and electrode effects or the accumulation of nano-sized capacitors. When 1.0 wt.%  $\text{Cu}_2\text{Zr}_3\text{O}_7$  is loaded into HDPE, the dielectric constant increases, showing that the surface of the particles serves as mini-capacitor inside the composites and that the majority of nano  $\text{Cu}_2\text{Zr}_3\text{O}_7$  particles is well-dispersed in the polymer matrix.

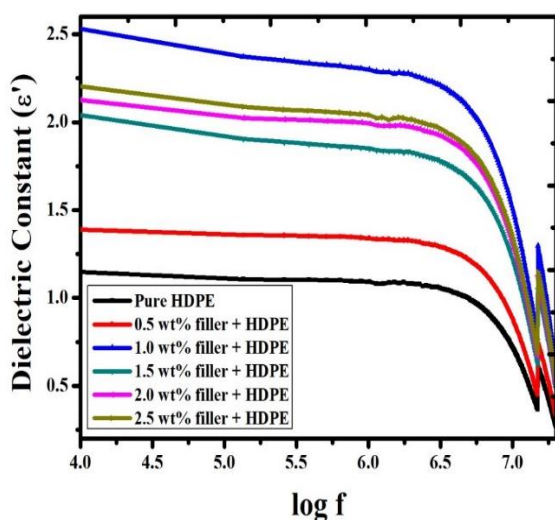


**Fig. 10: Dielectric constant of nano  $\text{Cu}_2\text{Zr}_3\text{O}_7$  - HDPE composites as a function of log frequency**

Fig. 10 further shows that when the test frequency increases to 10 MHz, the true permittivity decreases, but this effect is less pronounced for smaller filler loadings. Because HDPE is a non-polar material, the dielectric constant is not changed by frequency in the case of pure HDPE and only the nano filler contributes to such phenomenon, exhibiting the same trend in all samples investigated.<sup>13</sup> Dielectric distribution is responsible for the drop in dielectric constant with frequency.

**Loss tangent:** Fig. 11 shows the fluctuation in loss tangent ( $\tan\delta$ ) of the nano  $\text{Cu}_2\text{Zr}_3\text{O}_7$  - HDPE composite sheet as a function of frequency. It can be seen that the  $\tan\delta$  reduces rapidly at first and then gradually with increasing frequency in the range of 4 Hz to 1 MHz. The loss in  $\tan\delta$  is more pronounced at lower nanofiller amounts. The  $\tan\delta$  decreases as the loss storage ratio decreases, meaning that the composite becomes more insulating at higher frequencies. Moreover, in the accumulation field, the capacitance of the nano  $\text{Cu}_2\text{Zr}_3\text{O}_7$  - HDPE composite sheet is primarily influenced by the dielectric properties of the bulk insulator at high frequencies. This indicates that the behavior of the composite at higher frequencies is mainly determined by the characteristics of the insulating matrix, particularly in the region where the nanofiller is located.

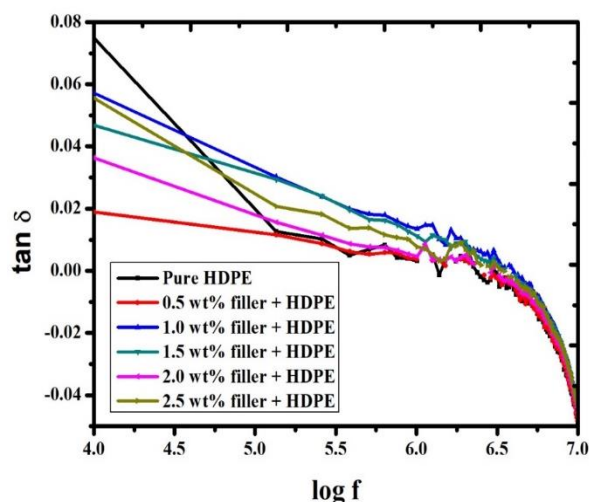


**Fig. 11: Loss tangent of nano  $\text{Cu}_2\text{Zr}_3\text{O}_7$  - HDPE composites as a function of log frequency**

**Electrical Conductivity:** The electrical conductivity results of the nano  $\text{Cu}_2\text{Zr}_3\text{O}_7$  - HDPE composite as a function of frequency with varying filler loadings are shown in fig. 12. It can be seen that the electrical conductivity of the composite improves at higher frequencies when compared to pure HDPE. At lower frequencies, however, there is no substantial relationship between frequency and conductivity and direct current distance is the determining factor. Low electrical conductivity is common in polymer matrices such as HDPE, especially at low filler concentrations. At higher frequency ranges, the overlap frequency, which shows other characteristic behaviour, is typically analysed. The conductivity of neat HDPE exhibits high dispersion which can be related to the low conductivity of the pure material itself.

The slope of the conductivity curve varies for greater filler loadings and higher frequency regions, as seen in fig. 12. This indicates that at higher frequencies, conductivity increases with increased filler loading. It is expected that there is a relationship between conductivity and filler loading where the nano  $\text{Cu}_2\text{Zr}_3\text{O}_7$  particles, being more conductive material than the insulating HDPE matrix, improve the composite's overall electrical characteristics.

The incorporation of nano fillers in the composite results in improved electrical conductivity which ranges from  $1.75 \times 10^{-6}$  to  $0.5 \times 10^{-7}$  S/m and can be beneficial for a variety of applications.

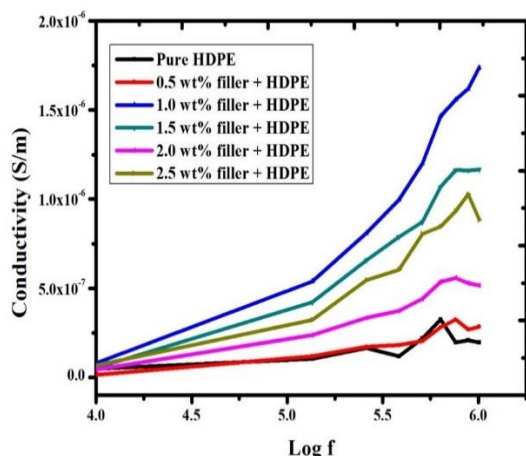


**Fig. 12: Electrical conductivity of nano  $\text{Cu}_2\text{Zr}_3\text{O}_7$  - HDPE composites as a function of log frequency**

## Conclusion

The main outcomes of the study can be stated as follows: The solution combustion investigate was used to successfully synthesise copper zirconium oxide nanoparticles from three different fuel sources (glycine, urea and sugar). The average particle size of synthesised copper zirconium oxide was 80 nm for glycine, 120 nm for urea and 130 nm for sugar, according to SEM examination. The presence of zirconium oxide and copper oxide peaks in the compound was confirmed by XRD analysis, showing the synthesis of copper zirconium oxide via the combination of copper oxide and zirconium oxide. EDX examination revealed the presence of copper, zirconium and oxygen in the synthesised nanoparticles. The composite's tensile strength was increased, as evidenced by a 34% increase in Young's modulus compared to blank HDPE for the sample with 1.5 wt% nanofiller loading.

The composite's dielectric constant decreased as frequency and nanofiller concentration increased, with the exception of the sample with 1% filler loading, which had the highest dielectric constant. The composite's loss tangent dropped first and then gradually with increasing frequency, indicating a reduction in loss storage ratio and enhanced insulating behaviour at higher frequencies. The electrical conductivity of the composite improved at higher frequencies and filler loadings, suggesting a relationship between filler loading and conductivity enhancement. Overall, the results indicate that adding copper zirconium oxide nanoparticles to HDPE can improve mechanical and electrical properties with possible uses in a variety of industries.

## References

1. Anandraj J. and Joshi G.M., Fabrication, performance and applications of integrated nanodielectric properties of materials—a review, *Composite Interfaces*, **25**(5-7), 455-489 (2018)

2. Alsayed Z., Awad R. and Badawi M.S., Thermo-mechanical properties of high-density polyethylene with zinc oxide as a filler, *Iranian Polymer Journal*, **29**, 309-320 (2020)

3. Bakis C.E., Haluza R.T., Bartolai J., Kim J.J. and Simpson T.W., Assessment of anisotropic mechanical properties of a 3D printed carbon whisker reinforced composite, *Advanced Composite Materials*, **28**(5), 545-560 (2019)

4. Dua M. and Mertiny P., Comparison of the Elastic Modulus of Elastomer Clay Nanocomposites Predicted by Various Mechanical Models, In Canadian Society for Mechanical Engineering International Congress (2021)

5. Elmahdy M., Abouelmagd G. and Mazen A.A.E., Microstructure and properties of Cu-ZrO<sub>2</sub> nanocomposites synthesized by in situ processing, *Materials Research*, **21**, 1-11 (2017)

6. Gunes I., Uygunoglu T. and Çelik A.G., Tribological properties of fly ash blended polymer composites, *Matéria (Rio de Janeiro)* (2021)

7. Gupta N., Gupta S.M. and Sharma S.K., Carbon nanotubes: Synthesis, properties and engineering applications, *Carbon Letters*, **29**, 419-447 (2019)

8. He Y. and Yu Z., Thermal stability and dynamic mechanical behavior of functional multiphase boride ceramics/epoxy composites, *Journal of Polymer Engineering*, **39**(6), 508-514 (2019)

9. Hu C., Sun J., Long C., Wu L., Zhou C. and Zhang X., Synthesis of nano zirconium oxide and its application in dentistry, *Nanotechnology Reviews*, **8**(1), 396-404 (2019)

10. Huang X., Sun B., Zhu Y., Li S. and Jiang P., High-k polymer nanocomposites with 1D filler for dielectric and energy storage applications, *Progress in Materials Science*, **100**, 187-225 (2019)

11. Koteswara Rao J., Abhishek R., Satyanarayana S.V., Madhu G. M. and Venkatesham V., Influence of cadmium sulfide nanoparticles on structural and electrical properties of polyvinyl alcohol films, *Express Polymer Letters*, **10**(11), 883-894 (2016)

12. Lashari N. and Ganat T., Emerging applications of nanomaterials in chemical enhanced oil recovery: Progress and perspective, *Chinese Journal of Chemical Engineering*, **28**(8), 1995-2009 (2020)

13. Lu X., Tong Y., Talebinezhad H., Zhang L. and Cheng Z.Y., Dielectric and energy-storage performance of Ba<sub>0.5</sub>Sr<sub>0.5</sub>TiO<sub>3</sub>-SiO<sub>2</sub> ceramic-glass composites, *Journal of Alloys and Compounds*, **745**, 127-134 (2018)

14. Marín-Genescà M., García-Amorós J., Mujal-Rosas R., Massagués L. and Colom X., Study and characterization of the dielectric behavior of low linear density polyethylene composites mixed with ground tire rubber particles, *Polymers*, **12**(5), 1075 (2020)

15. Mujeeb A., Lobo A.G., Antony A.J. and Ramis M.K., An experimental study on the thermal properties and electrical properties of polylactide doped with nano aluminium oxide and nano cupric oxide, *INAE Letters*, **2**, 145-151 (2017)

16. Nasr G., Mohamed T. and Khalil R., Dynamic Mechanical and Dielectric Properties of Fly Ash/(Polystyrene/Low-Density Polyethylene) Composites, *Materials Performance and Characterization*, **9(1)**, 654-664 (2020)
17. Peacock A., Handbook of polyethylene: structures: properties and applications, CRC Press (2000)
18. Phromviyo N., Chanlek N., Thongbai P. and Maensiri S., Enhanced dielectric permittivity with retaining low loss in poly (vinylidene fluoride) by incorporating with Ag nanoparticles synthesized via hydrothermal method, *Applied Surface Science*, **446**, 59-65 (2018)
19. Rao J.K., Raizada A., Ganguly D., Mankad M.M., Satayanarayana S.V. and Madhu G.M., Investigation of structural and electrical properties of novel CuO–PVA nanocomposite films, *Journal of Materials Science*, **50**, 7064-7074 (2015)
20. Salih S.E., Preparation and Characterization Advanced Polymer Blend Nano Composite Materials, *Iraqi Journal of Mechanical and Material Engineering*, **17(4)**, 625-638 (2017)
21. Sinha Ray S. and Ojijo V., A brief overview of layered silicates and polymer/layered silicate nanocomposite formation, *Processing of Polymer-Based Nanocomposites: Introduction*, **277**, 57-86 (2018)
22. Satapathy S., Development of value-added composites from recycled high-density polyethylene, jute fiber and flyashcenospheres: Mechanical, dynamic mechanical and thermal properties, *International Journal of Plastics Technology*, **22**, 386-405 (2018)
23. Wang J., Yin W., He X., Wang Q., Guo M. and Chen S., Good biocompatibility and sintering properties of zirconia nanoparticles synthesized via vapor-phase hydrolysis, *Scientific Reports*, **6(1)**, 1-9 (2016)
24. Zha J.W., Zheng M.S., Fan B.H. and Dang Z.M., Polymer-based dielectrics with high permittivity for electric energy storage: A review, *Nano Energy*, **89**, 106438 (2021).

(Received 29<sup>th</sup> May 2023, accepted 28<sup>th</sup> June 2023)